

Polarization of Charge-Transfer Bands and Rectification in Hexadecylquinolinium 7,7,8-Tricyanoquinodimethanide and Its Tetrafluoro Analog

Andrei Honciuc,[†] Akihiro Otsuka,^{†,‡} Yu-Hsiang Wang,[†] Samuel K. McElwee,[†] Stephen A. Woski,[†] Gunzi Saito,[§] and Robert M. Metzger^{*,†}

Laboratory for Molecular Electronics, Chemistry Department, University of Alabama, Tuscaloosa, Alabama 35487-0336, Research Center for Low-Temperature and Materials Sciences, Kyoto University, Sakyo-ku, Kyoto 606-8502, Japan, and Division of Chemistry, Graduate School of Science, Kyoto University, Sakyo-ku, Kyoto 606-8502, Japan

Received: November 28, 2005; In Final Form: April 24, 2006

A Langmuir–Blodgett (LB) multilayer film of the unimolecular rectifier hexadecyl- γ -quinolinium-7,7,8-tricyanoquinodimethanide ($C_{16}H_{33}\gamma Q-3CNQ$) has two distinct polarized charge-transfer bands, one at lower film pressures (28 mN m⁻¹) with a peak at 530 nm, due to an intramolecular charge transfer or intervalence transfer (IVT); past the collapse point (32 to 35 mN m⁻¹), this band disappears, and a new intermolecular charge-transfer band appears with peak at 570 nm. An LB multilayer film of the tetrafluoro analogue, hexadecyl- γ -quinolinium-2,3,5,6-tetrafluoro-7,7,8-tricyanoquinodimethanide ($C_{16}H_{33}\gamma Q-3CNQF_4$) shows, for all film pressures, only one IVT band with a peak at 504 nm; when sandwiched between gold electrodes, ($C_{16}H_{33}\gamma Q-3CNQF_4$) is also an LB monolayer electrical rectifier.

Introduction

Unimolecular rectifiers have received considerable attention recently because of the perceived desirability of organic nanocomputers.^{1–3} These rectifiers should be reliable over many cycles of measurement but often are not.² We confirmed unimolecular rectification in hexadecyl- γ -quinolinium 7,7,8-tricyanoquinodimethanide, $C_{16}H_{33}\gamma Q-3CNQ$ (Figure 1, structure 1), sandwiched first between Al electrodes at room temperature,^{4,5} and between 105 and 370 K,⁶ then at room temperature between Au electrodes.^{7,8} The spectroscopy of 1^{9,10} and theoretical calculations^{11–15} confirmed conclusively that its ground state is the very polar zwitterion $D^+-\pi-A^-$ (D^+ is the quinolinium moiety, and A^- is the tricyano-quinodimethanide moiety), while the first excited state has the less polar structure $D^0-\pi-A^0$.

However, an issue is whether the ground state is exactly $D^{+1.0}-\pi-A^{-1.0}$, and the excited-state $D^{0.0}-\pi-A^{0.0}$, or whether we should also consider intermediate ionicities $D^{+\rho}-\pi-A^{-\rho}$, ($\rho \geq 0.8$) for the ground state and $D^{+\rho'}-\pi-A^{-\rho'}$ ($\rho' \leq 0.2$) for the excited state.^{14,15} A recent theoretical calculation found $\rho \approx 0.9$ and that ρ depends slightly on the solvent.¹⁴ In light of this, using in the synthesis the perfluorinated stronger one-electron acceptor TCNQF₄, rather than the strong acceptor TCNQ, may increase the value of ρ , and decrease that of ρ' , and the consequences for molecular rectification may be interesting: that possibility has now been tested.

There is an intramolecular charge-transfer (ICT) or intervalence band (IVT), which is strongly hypsochromic in solution⁹ and was believed to be involved in the rectification. The current–voltage (I – V) plot for a monolayer of 1, sandwiched between metal electrodes, has an onset of significant electrical asymmetry between +0.8 and +1.5 V between Al electrodes,⁴ and at 1.6 V between Au electrodes.⁸

Many homologues of $C_{16}H_{33}\gamma Q-3CNQ$ have been studied^{16,17} and restudied.¹⁸ For shorter alkyl chains, in the structure $C_nH_{2n+1}\gamma Q-3CNQ$, where $n \leq 14$, the Z-type LB multilayer orientation is no longer preferred, presumably because the van der Waals intermolecular attraction between adjacent molecules, facilitated by the alkyl “tail”, no longer dominates over the dipole–dipole repulsion between the largely zwitterionic chromophores.¹⁷

A crystal structure determination of a microcrystalline sample of 1 was not possible;⁴ thus, the angle θ between the least-squares plane of the quinolinium rings and the tricyanoquinodimethanide rings could not be determined.⁴ Calculations suggested^{4,11} that if the quinolinium and tricyanoquinodimethanide rings are mutually orthogonal ($\theta = 90^\circ$), then the IVT should vanish, and the ground-state dipole moment should be a maximum. If $\theta = 0$, then the two states 1 and 1' would be degenerate, and IVT would disappear; however, steric hindrance would prevent $\theta = 0$. In the related crystal structure of α -picolinium tricyanoquinodimethanide (or α -picolyl tricyanoquinodimethane) (Figure 1, structure 2) $\theta = 30.13^\circ$ was measured.¹⁹ The question is whether such a twist angle is replicated in the series of molecules $R\gamma Q-3CNQ$, $R = C_nH_{2n+1}$ (Figure 1, structure 3). Recently, the crystal structure of decyl- α -quinolinium tricyano-quinodimethanide, $C_{10}H_{21}\alpha Q-3CNQ$, 4, was determined:¹⁸ the ground state is zwitterionic, and the twist angle is $\theta = 31.40^\circ \pm 0.04^\circ$.

Some other rectifiers have been characterized.^{20–22} In the hope of driving the ionic state to an even higher degree of charge separation,¹⁵ the tetrafluoro analogue of 1, namely, hexadecyl- γ -quinolinium-2,3,5,6-tetrafluoro-7,7,8-tricyanoquinodimethanide ($C_{16}H_{33}\gamma Q-3CNQF_4$), (Figure 1, structure 5) was synthesized again. The optical properties of LB multilayers of 5 have been reported previously.¹⁶ Because the tetrafluoro analogue of TCNQ has an estimated electron affinity that is ~ 0.4 eV greater than unfluorinated TCNQ,²³ it is likely that the LUMO of 5 is somewhat below the LUMO of 1. If this LUMO is involved in

* Corresponding author. E-mail: rmetzger@bama.ua.edu.

[†] University of Alabama.

[‡] Center for Low Temperature and Materials Sciences, Kyoto University.

[§] Division of Chemistry, Graduate School of Science, Kyoto University.

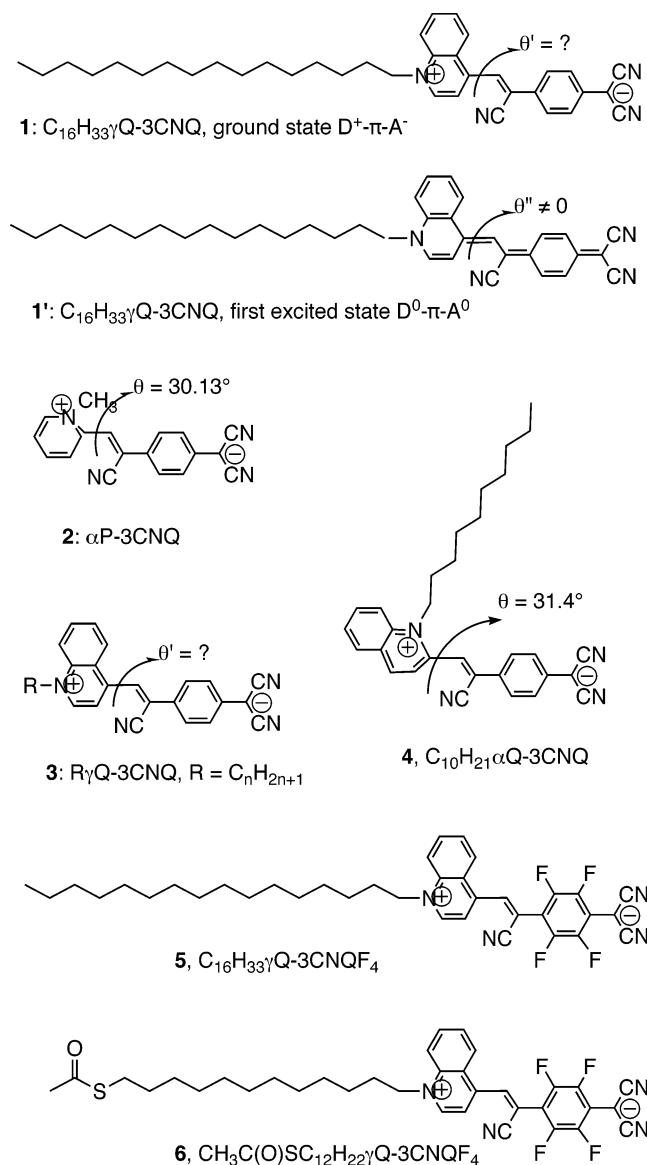


Figure 1. Structures 1–6.

the rectification process, as it was assumed⁴ to be for **1**, then the onset of asymmetrical current in **5** may occur at a lower bias than for **1**.

In addition, an analogue of **5** was also synthesized, which should have been suitable for “self-assembled” monolayers (thiolates chemisorbed to Au): thioacetyl-dodecyl- γ -quinolinium 2,3,5,6-tetrafluoro-7,7,8-tricyanoquinodimethanide, $CH_3C(O)-SC_{12}H_{22}\gamma Q-3CNQF_4$ (Figure 1, compound **6**).

The relative location, intensity, and polarization of the IVT band in LB films of **1** and **5** may be of great relevance, so UV-vis spectra of LB multilayers of both **1** and **5** were measured using polarized light. Some previous results for **1**^{4–9} and **5**¹⁶ are reinterpreted below, in light of new evidence.

Experimental Methods

The synthetic details are given in the Supporting Information.

NMR spectra were measured using Bruker 360 MHz and JEOL 400 MHz spectrometers. MALDI-TOF mass spectra were measured in the positive mode with 2,5-dihydroxybenzoic acid (DHB) as the matrix using a Bruker-Daltonics Reflex III MALDI-TOF spectrometer. The elemental analyses were performed by Atlantic Microlab, Inc.

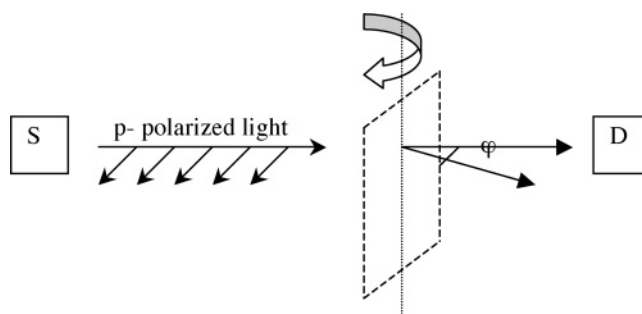


Figure 2. Schematic of the polarization experiment, performed with p-polarized light. S and D are the source and the detector, respectively. The light leaving the source, S, is polarized in the horizontal plane (in and out of the plane of this diagram). The LB film was deposited on the quartz in the vertical direction (up and down in the plane of this diagram). The planar quartz substrate bearing the LB multilayer (denoted by the dashed parallelogram) is rotated so that the normal to its plane makes an angle φ (0 to 180°) with the incident polarized light (at $\varphi = 0^\circ$ the normal to the quartz substrate is along the vector from S to D).

Cyclic voltammograms were measured using a PAR 273 electrochemical potentiostat (EG&G instruments). A four-neck cell, equipped with a Pt disk working electrode, a Pt wire counter electrode, and a saturated calomel electrode (SCE) as the reference electrode, was used under an inert Ar atmosphere. Measurements were performed on solutions (10^{-3} and 5×10^{-3} M in distilled CH_2Cl_2) with 0.1 M tetrabutylammonium hexafluorophosphate as a supporting electrolyte.

Electronic absorption spectra were recorded at room temperature on a Cary 50 ultraviolet–visible (UV–vis) single-beam spectrophotometer, using a quartz cuvette with a 1 cm path length, and also on an LB multilayer film deposited on a quartz substrate as a function of temperature, using a heating gun introduced into the sample compartment, a type-K (chromel–alumel) thermocouple placed next to the substrate, and an Omega Model HH23 microprocessor-controlled thermometer. A polarization experiment was conducted (Figure 2): a linear polarizer was placed in front of the source, S, so that the electric vector was horizontal.

Langmuir (or Pockels–Langmuir) isotherms were measured at the air–water interface, and Langmuir–Blodgett (LB) monolayers and multilayers were deposited on solid substrates, using a NIMA (Coventry, U.K.) model 622 computer-controlled film balance, in a room with HEPA-filtered air, under a green safelight, with ultrapure water (Barnstead Easypure LF, 18.3 MΩ cm) as the subphase, and dropping onto the water surface a ~ 0.2 mg/mL solution of compound **5** in (7:3) CCl_2CHCl/CH_3CN . To duplicate previous results,¹⁶ alternate-layer deposition was also used to force the transfer of successive monolayers of **5** on the upstroke only, thus forming Z-type multilayers of **5**. The substrate dipping speed was always kept at 4 mm min^{-1} , and the compression velocity was kept at $50 \text{ cm}^2 \text{ min}^{-1}$.

Core level and valence-band X-ray photoelectron spectroscopy (XPS) studies on thick cast films of both **1** and **5** were performed with a Kratos Axis 165 spectrometer in a chamber with a base pressure of $\sim 3 \times 10^{-10}$ Torr. Monochromatic Al K α radiation at 1486.6 eV was used as the excitation source, and a two-point correction method was used to correct for sample charging.

Spectroscopic ellipsometry was performed using a Woolam spectroscopic ellipsometer, with a Cauchy model fit to the data.

Infrared spectra and grazing-angle reflection-absorption infrared spectra (RAIRS) were measured on a Bruker IFS-88 FTIR spectrophotometer equipped with liquid-nitrogen-cooled MCT

wide-band detector. For each spectrum, a 1000-scan interferogram was collected in a single-beam mode with 4 cm^{-1} resolution. The incident angle of the p-polarized light was set to 85° relative to the substrate normal.

The Volta (Kelvin) electrostatic potential difference between air, the monolayer of **5**, and a 150-nm-thick Au substrate was measured at room temperature under a blanket of N_2 gas using a Monroe "Isoprobe" 162 electrostatic voltmeter.

The assembly of "Au | monolayer | Au" sandwiches started with a Si wafer, which was first covered by an adhesion layer (15 nm Cr) and then covered by 150 nm of Au in an Edwards EL306A evaporator (chamber base pressure below 1.0×10^{-7} mbar) at 200°C and an evaporation rate of 0.1 nm s^{-1} . Before use, each gold-coated silicon substrate was hydrogen flame-annealed for about 1.5 min to remove any organic material on the gold surface and also to improve the gold terracing.

LB monolayers of **1**, **5**, or **6** were then deposited atop the Au (kept hydrophilic by minimal exposure to air, and exposed to UV/ozone immediately before use). The SAM monolayer of **6** was exposed to ammonia for 15 min after LB transfer to aid in forming the gold–thiolate bond and removing the acetate leaving-group. The LB monolayer of **1**, **5**, or **6** atop Au was dried in a vacuum desiccator for 2 days in the presence of P_2O_5 .

Using the Edwards EL306 evaporator, a pattern of 400 gold electrode pads, 0.283 mm^2 in area and about 33 nm thick, was evaporated through a contact mask onto the unimolecular LB layer by the "cold-gold" technique described elsewhere⁸ but with recent improvements: The gold deposition was monitored continuously with the first quartz-crystal thickness monitor, oriented towards the source, while a nominal 370 nm of Au was deposited on surfaces facing the source directly. A liquid-nitrogen-cooled finger was used as the sample mount. The sample was mounted on the finger surface, facing away from the Au source, to avoid direct heating of the substrate and damaging the monolayer.⁸ A second quartz-crystal thickness monitor was oriented in the same direction as the sample (which is shielded from the source by the cold finger). The gold thickness on the sample was $\sim 33\text{ nm}$. The temperature at the sample was monitored during gold deposition: it never exceeded 170 K.

After removal of the sample from the evaporator, "soft" electrical contact to the bottom Au electrode and to each of the top Au pads was made by a Ga/In eutectic drop, using micromanipulators. I – V curves of the sandwiched monolayers, enclosed in a Faraday cage, were measured using a Keithley 236 Source Measure Unit, controlled by a personal computer (PC).

Molecular Properties. The cyclic voltammogram of **5** (Figure 3) resembles that of compound **1**: the first reduction of **5** occurs at -0.492 V (reduction) and -0.389 V (reoxidation) versus SCE, so $E_{1/2} = -0.440\text{ V}$ versus SCE; this reduction is shifted by $+0.073\text{ V}$ from the value $E_{1/2} = -0.513\text{ V}$ versus SCE reported for compound **1**.⁴ In contrast, **5** starts to oxidize irreversibly only at 0.834 V versus SCE, while compound **1** does so at 0.487 or 0.49 V versus SCE.⁴

The relative energies of compound **5** were computed, as a function of the torsion angle θ , at the semiempirical PM3 level (but using a CH_3 group instead of the $\text{C}_{16}\text{H}_{33}$ group), with the following results: a global minimum at $\theta = 25$ to 30° ($\Delta H \equiv 0$), a local maximum at $\theta = -10^\circ$ ($\Delta H = 3.2\text{ kcal/mol}$), a local minimum at $\theta = -30$ to -35° ($\Delta H = 2.5\text{ kcal/mol}$), and a local maximum at $\theta = 90^\circ$ ($\Delta H = 5.1\text{ kcal/mol}$) (see Supporting Information, Figure A). Room temperature is equivalent to $0.025\text{ eV} = 0.6\text{ kcal/mol}$; therefore, several rotamers of **5** should be

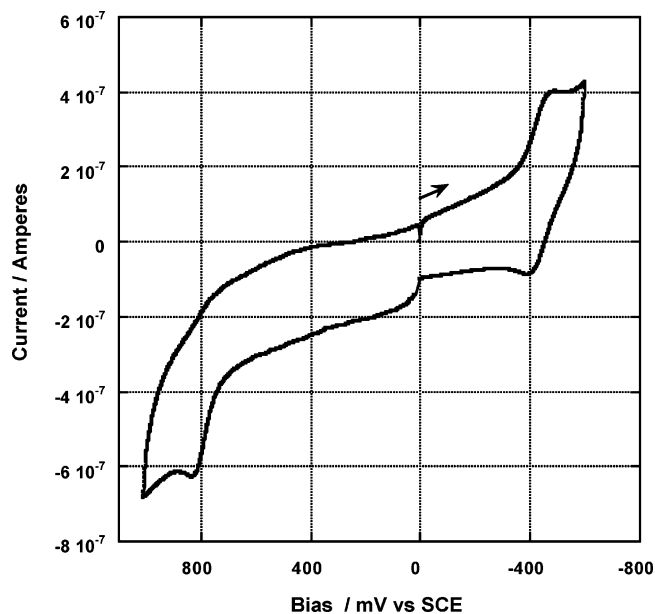


Figure 3. Cyclic voltammogram of **5**.

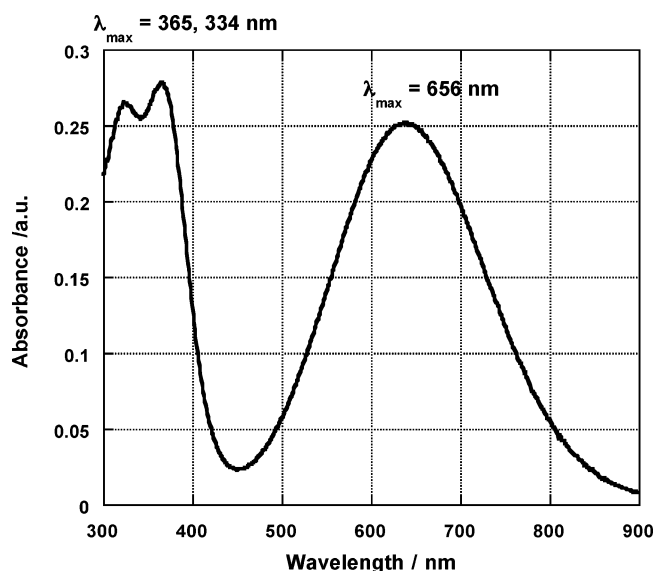


Figure 4. UV-vis spectrum of a solution of **5** in (7:3) $\text{CCl}_2\text{CHCl}/\text{CH}_3\text{CN}$ shows an intense CT band with maximum at 656 nm.

accessible. The total calculated molecular lengths of **1** and **5** are the same: 33 \AA .⁴

Spectroscopy. The UV-vis spectrum of compound **5** in a 7:3 volume ratio of $\text{CCl}_2\text{CHCl}/\text{CH}_3\text{CN}$ (a blue solution) is shown in Figure 4: the peak at $\lambda_{\text{max}} = 656\text{ nm}$ is presumed to be an IVT.

Solvatochromism studies, similar to those undertaken for **1**,⁹ were not done for **5** because of its limited solubility in other solvents. Because the UV-visible spectrum of LB films of **1**, as discussed below, differs considerably from the spectra reported previously,^{4,9,16,17} and because **1** is known to decompose after two years of storage in a refrigerator, **1** was resynthesized and its solution spectrum was remeasured in (7:3) $\text{CHCl}_3/\text{CH}_3\text{CN}$; an intense IVT peak ($\lambda_{\text{max}} = 800\text{ nm}$) was seen, as expected. The spectrum was also measured, after adding either stoichiometric or vastly excessive amounts of the base ($\text{CH}_3\text{CH}_2\text{N}_3$), which should remove any adventitious acidic protons from **1**. Except for dilution effects, no changes in the spectrum were seen. Therefore, compound **1** was deemed to be acid-free, as prepared.

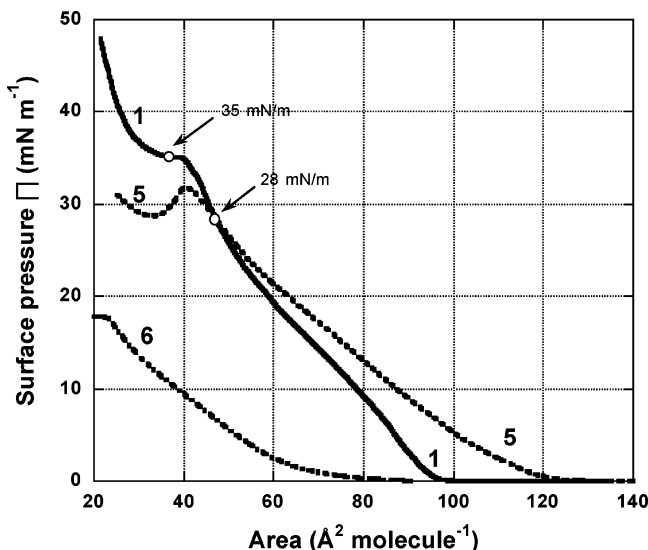


Figure 5. Pressure–area isotherm of **1** at 14 °C (subphase pH = 7), **5**, and **6**. The two marked points for the isotherm of **1** correspond to the two pressures (28 and 35 mN m^{−1}), at which Langmuir–Blodgett films were transferred, below and just beyond the phase transition or collapse point at 32 mN m^{−1}.

TABLE 1: Surface Pressures Π (± 2 mN m^{−1}) and Molecular Areas A (± 1 Å² molecule^{−1}) for Pockels–Langmuir Films at the Air–Water Interface at Various Points along the Pressure–Area Isotherms at 17 °C (measured at 20 °C in ref 4)

molecule	A_0 Å ²	Π_1 mN m ^{−1}	A_1 Å ²	Π_2 mN m ^{−1}	A_2 Å ²	Π_3 mN m ^{−1}	A_3 Å ²	Π_c mN m ^{−1}	A_c Å ²
1	95	20 ⁴	70 ⁴	28	48	31	43	32	40
5	122							32	40
6	90					17	23	18	22

LB Film Properties. The pressure–area isotherms of **1**, **5**, and **6** are shown in Figure 5; relevant data are collected in Table 1.

The initial area, A_0 , is the area where the surface pressure, Π , starts to depart from zero. At a surface pressure $\Pi_c = 32$ mN m^{−1} (which can vary between 31 and 35 mN m^{−1}), both **1** and **5** undergo a significant phase transition, or a collapse, which is particularly dramatic for **5**. At this point, the areas are $A_c = 40$ Å² molecule^{−1} for both **1** and **5**. In previous work for **1**, Langmuir–Blodgett (LB) transfer was done at $\Pi_1 = 20$ mN m^{−1} and $A_1 = 70$ Å² molecule^{−1} for **1** at 293 K;⁴ here we found $A_1 = 60$ Å² molecule^{−1} at $\Pi_1 = 20$ mN m^{−1} at 287 K.

We will show below that there is a significant change in the optical properties for LB films transferred somewhat before versus just beyond the collapse point. The LB transfer of multilayers of **1** onto hydrophilic surfaces (Al, Au) at all pressures is, as before,^{4,8} Z-type (acentric) for all layers.

In contrast, the transfer of multilayers of **5** is Z-type (the more polar dicyanomethanide group lies closer to a hydrophilic substrate than the nonpolar hexadecyl group) only for the first layer but Y-type (centrosymmetric) thereafter: at a dipper speed of 4 mm min^{−1}, the transfer ratios are 100%, 80%, 100%, 80%, and so forth.

The pressure–area isotherm of **6** yields the area at zero pressure $A_0 = 90 \pm 2$ Å² molecule^{−1}; the isotherm rises linearly with pressure, until collapse occurs at a surface pressure $\Pi_c = 17 \pm 1$ mN m^{−1} and at an unacceptably low $A_c = 22$ Å² molecule^{−1}. The chosen transfer pressure for **6** was $\Pi_3 = 17$ mN m^{−1} (for which $A_3 = 23$ Å² molecule^{−1}).

The film thickness for a monolayer of **1** on quartz, measured by spectroscopic ellipsometry, is 24.0 ± 1.0 Å for the film

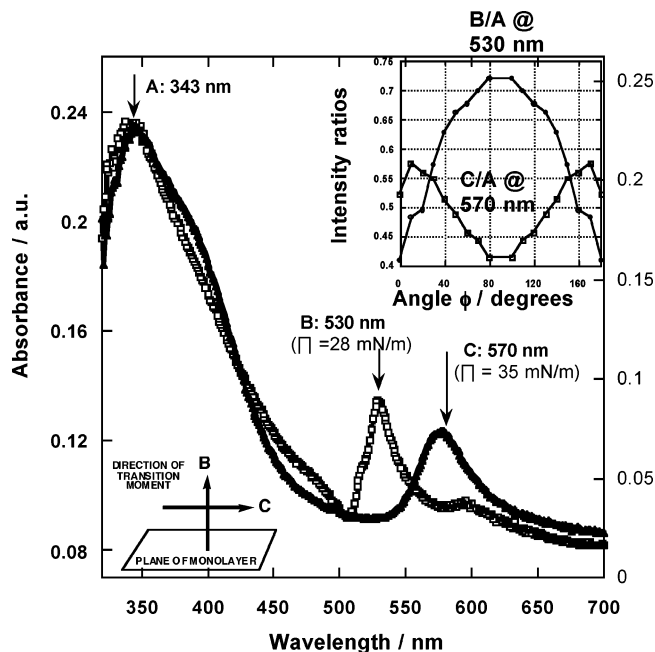


Figure 6. Polarized UV–vis spectra of 14 monolayers of **1**, deposited on quartz substrates. The spectrum with open squares (monolayers transferred at a pressure of 28 mN m^{−1}) shows a peak (A) at 343 nm and a peak (B) at 530 nm; the spectrum with closed triangles (monolayers transferred at 35 mN m^{−1}) has peaks A at 343 nm and C at 570 nm. The two spectra were measured with angle $\varphi = 0^\circ$, and were normalized so as to have the same intensity of peak A. Top right inset: Polarization of the peak ratios B/A and C/A for 14 layers of **1**, as a function of the angle φ : the intensity ratio B/A has a relative maximum of 0.73 at $\varphi = 80\text{--}90^\circ$, and a relative minimum of 0.41 at both $\varphi = 0^\circ$ and $\varphi = 180^\circ$; the intensity ratio C/A has a minimum of 0.42 at $\varphi = 80\text{--}90^\circ$, and a maximum of 0.53 at both $\varphi = 0^\circ$ and $\varphi = 180^\circ$. Bottom left inset: depiction of direction of transition moment vectors for bands C and B, relative to the plane of the monolayer.

transferred at 28 mN m^{−1}, and slightly larger (25.6 ± 1.0 Å) for the film transferred at 35 mN m^{−1}, compared to the literature value⁹ of 22.0 ± 1.0 Å for films transferred at 25 mN m^{−1}: the film is slightly thicker for a monolayer of **1** transferred at the higher pressure. The monolayer of **5** transferred at 28 mN m^{−1} has a thickness of 24.0 ± 1.0 Å, again by spectroscopic ellipsometry.

If the molecular length of both **1** and **5** is taken to be 33 Å,⁴ then the molecules of **1** are tilted by $\cos^{-1}(24.0/33) = 44^\circ$ at 28 mN m^{−1} and by $\cos^{-1}(25.6/33) = 29^\circ$ at 35 mN m^{−1}, while the molecules of **5** are tilted by $\cos^{-1}(24.0/33) = 44^\circ$ at 28 mN m^{−1}.

Multilayers of **5** on quartz are colorless to the naked eye, while multilayers of **1** are blue-green.

The multilayer films of **1** deposited on quartz at 28 and at 35 mN m^{−1} exhibit markedly different optical properties (Figure 6). There is a peak (A) at 343 nm, which is also seen in solution, and is not solvatochromic: this peak is due to some intramolecular excitation, that does not involve the zwitterionic state, and can be used as an intensity reference. Then there is a peak (B) at 530 nm (2.34 eV), which occurs for $\Pi = 28$ mN m^{−1} (below the collapse point), but is not seen for $\Pi = 35$ mN m^{−1} (beyond the collapse point). Finally, there is a peak (C) at 570 nm (2.18 eV), which occurs only for $\Pi = 35$ mN m^{−1} (beyond the collapse point) but is not seen at $\Pi = 28$ mN m^{−1} (below the collapse point). The relatively low intensity of the 530 and 570 nm bands in Figure 6, compared to previous experience,^{4,9,16,17} and their pressure dependence suggested that polarization studies be undertaken.

The inset of Figure 6 shows that, as the sample is rotated by an angle φ (Figure 2), peak A is unchanged, but the intensity ratio B/A has a broad maximum for $\varphi = 80$ to 90° , that is, peak B at 530 nm is most intense when the electric vector is normal to the quartz surface: this suggests that the sample-average transition moment responsible for the B peak at 530 nm is normal to the monolayer plane. In contrast, peak A is unchanged, but the intensity ratio C/A has a broad minimum at $\varphi = 80$ to 90° , and a broad maximum for $\varphi = 0$ to 10° , that is, the sample-average transition moment for the band peak C at 570 nm lies in the plane of the film. The spectra of Figure 6 contrast with the published spectrum (Figure 5 of ref 4): the peak at 570 nm was attributed⁴ to an LB film deposited at 14°C and 20 mN m^{-1} , while Figure 6 shows that the intense band at 570 nm is visible only if the deposition pressure, 35 mN m^{-1} , is beyond the collapse point, and the angle φ is close to 0° . The film pressure for the multilayer of Figure 5 of ref 4 must have been deposited on quartz beyond the collapse point.

A dilution of **1** with eicosanoic acid in 1:1 molar ratio, after transfer onto a quartz substrate, exhibited a mixed LB monolayer with an unchanged A band but no B or C bands at all. Band B also disappears if the deposition pressure for **1** is below 22 mN m^{-1} . If the spectra of Figure 6 are remeasured after several days, then the polarization of the B or C bands does not change.

Because the results of Figure 6 are surprisingly different from our own published results^{4,9} and from the results of Ashwell and co-workers^{16,17} (i.e., because the IVT peaks are much weaker than seen previously), some care was taken to make sure that there was no accidental protonation of the film, which is known to suppress the IVT,⁴ and decrease the B/A and C/A intensity ratios ("bleaching"): (i) exposure of the solution to triethylamine had no effect; (ii) exposure of the films to ammonia had no effect; (iii) making the pH of the aqueous subphase in the film balance basic had no effect; (iv) a fresh synthesis of **1**, followed by dissolving this fresh sample in several dropping solvents [tetrahydrofuran (freshly distilled and dried over sodium), or acetonitrile (distilled and dried over calcium hydride) plus NMR grade deuterated chloroform, or in acid-free deuterated acetonitrile (Cambridge Isotope Labs., 99.8 atom % pure) from a sealed ampule] brought about no change in the film spectra.

Figure B in the Supporting Information shows the polarization of the UV-vis spectra of a mixed multilayer (seven layers deposited at 28 mN m^{-1} , seven more deposited at 35 mN m^{-1}). If the absorption spectrum of the alternate film is remeasured after 48 hours, then the polarization of bands B and C is completely lost: the film probably acquires a more thermodynamically stable structure.

FTIR grazing-angle spectra of monolayers of **1** deposited at 28 and 35 mN m^{-1} are identical.

The optical data for **5** published previously claim that a solution of **5** in pure CH_3CN has an IVT maximum at $\lambda_{\text{max}} = 565\text{ nm}$ ($\log \epsilon = 2.20$),¹⁶ while a Z-type multilayer film of **5**, prepared by alternate-layer deposition, has an IVT maximum at $\lambda_{\text{max}} = 480\text{ nm}$ ($\log \epsilon = 2.59$).¹⁶ In contrast, we found that **5** is practically insoluble in pure CH_3CN , but a solution of **5** in (7:3) $\text{CCl}_2\text{CHCl}/\text{CH}_3\text{CN}$ has $\lambda_{\text{max}} = 656\text{ nm}$ (Figure 4).

In Y-type LB multilayers of **5** there is a strong (A) peak at 330 nm and a polarization-dependent peak (D) at 504 nm (2.46 eV), which is almost as intense as the (A) peak at $\varphi = 100^\circ$ (Figure 7). Peak D for **5** at 2.46 eV is shifted by 0.12 eV from peak B of **1**. The peak reported¹⁶ at 480 nm was not found.

The UV-vis spectrum of **5** shows some new features between 26 and 120°C (Figure C in the Supporting Information).

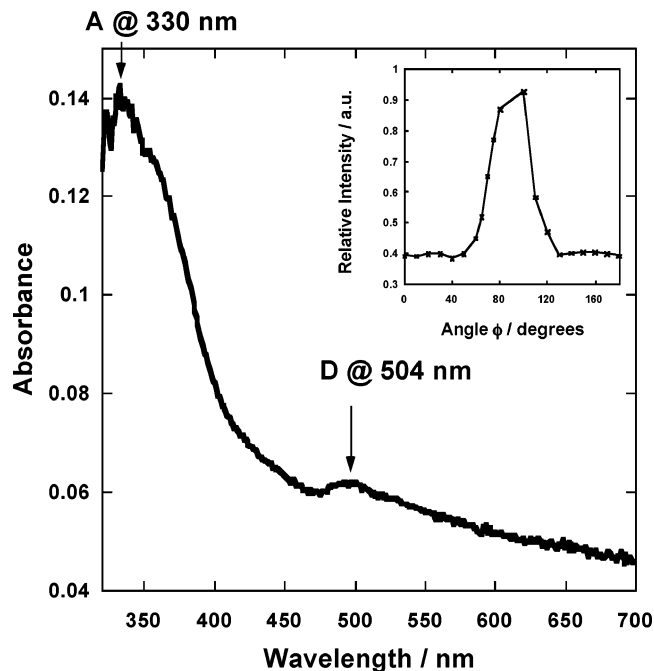


Figure 7. Polarized UV-vis spectrum of 14 Y-type LB monolayers of **5**, deposited on a quartz substrate. The spectrum, measured with angle $\varphi = 0^\circ$, shows a peak (A) at 330 nm and a peak (D) at 504 nm. Inset: Polarization of the peak ratio D/A for 14 layers of **5**, as a function of the angle φ : the intensity ratio D/A has a relatively sharp maximum of 0.92 at $\varphi = 100^\circ$, and a relative minimum of 0.41 at both $\varphi = 0^\circ$ and $\varphi = 180^\circ$.

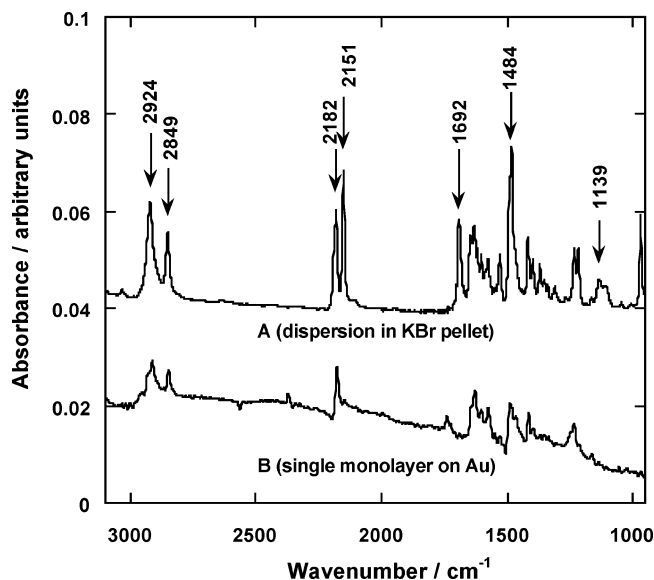


Figure 8. (A) FTIR spectrum of a dispersion of **5** in a KBr pellet. (B) Grazing-angle FTIR spectrum of a monolayer of **5** on Au.

The FTIR spectrum for a KBr pellet containing **5** and a grazing-incidence FTIR spectrum of a monolayer of **5** on Au are compared in Figure 8. In the KBr pellet of **5**, the CN peaks are at 2182 cm^{-1} (less intense) and 2151 cm^{-1} (more intense). For an LB monolayer of **5** on Au at grazing incidence, the more intense CN peak is at 2179 cm^{-1} (0.009 arbitrary units (a.u.)); the less intense peak is at 2149 cm^{-1} (0.002 a.u.).

For comparison, for a KBr pellet of **1** the peaks were at 2176 cm^{-1} (more intense) and 2136 cm^{-1} (less intense), plus a very weak IR peak at 2217 cm^{-1} , which was very intense in the Raman spectrum.¹⁰ For an LB monolayer of **1** on Au, the less intense peak was at 2177 cm^{-1} (0.0014 a.u.) and the more intense peak was at 2137 cm^{-1} (0.0024 a.u.).¹⁰

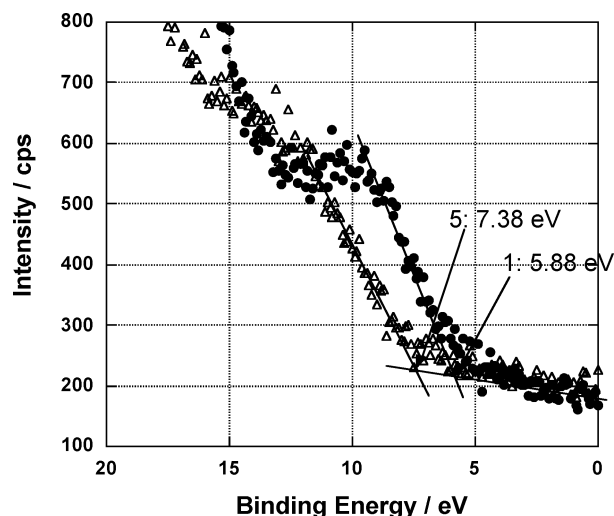


Figure 9. Valence-edge XPS spectrum of monolayer of **1** and **5** on an Au substrate: the band onset occurs at 5.88 eV for **1** but at 7.38 eV for **5**.

In summary, within instrumental error, the peak between 2176 and 2182 cm^{-1} is at the same position for both **1** and **5**, and is the more intense peak, except in the LB monolayer of **1**; the other peak in **1** (2137 or 2139 cm^{-1}) is at a significantly lower energy than that in **5** (2149 or 2151 cm^{-1}).

The IR peaks due to CN bands for solid samples in KBr pellets are often used to determine ionicity;²⁴ the highest-energy CN stretch occurs at 2222–2225 cm^{-1} (single peak) for the potent one-electron acceptor TCNQ but shifts²⁵ to 2196 cm^{-1} (second peak at 2182 cm^{-1} ; third peak at 2167 cm^{-1}) for the ionic salt $\text{K}^+\text{TCNQ}^{\bullet-}$. In comparison, this stretch occurs at 2226 cm^{-1} (second peak at 2214 cm^{-1}) for the even stronger electron acceptor TCNQF_4 and shifts²⁵ to 2212 cm^{-1} (second peak at 2192 cm^{-1}) for $\text{K}^+\text{TCNQF}_4^{\bullet-}$. We conclude that if **1** is zwitterionic in the ground state^{4,9,10,14} then **5** is also and that this zwitterionic state is preserved in the LB monolayer.

The valence-band edges were measured by XPS as 5.88 eV for a thick cast film of **1** on Au and 7.38 eV for a thick cast film of **5** on Au (Figure 9); these values are $E = -5.88$ eV versus $E(\text{vacuum})$ for **1** and -7.38 eV for **5**. Previously, the band edge of an LB monolayer of **1** was measured as 3.7 eV on Si, which, when corrected for the work function of Si (4.1 eV) became $E = -3.7 - 4.1 = -7.8$ eV versus $E(\text{vacuum})$.⁹ These measurements rely on either the initial slope (here) or the onset⁹ of a signal and can be somewhat uncertain. But the 1.5 eV difference in band edges between **1** and **5** is meaningful: it presumably mirrors a shift in the HOMO level (molecule **1** is easier to oxidize).

The Volta potential, or Kelvin probe potential, was measured for monolayers and multilayers of **5** at the interface between air and a quartz substrate covered with 150 nm of Au (Figure 10). Within experimental error, the centrosymmetric Y-type multilayers of **5** have the same potential: the build-up of multilayers, where the dipole of layer 2 is oriented opposite to layer 1, layer 3 opposite to layer 2, and so forth, presents only one net dipole layer. When the LB multilayer of **5** is forced to be Z-type by alternate-layer deposition, then the Volta potential changes monotonically with the number of layers, as the dipoles add with each successive monolayer deposition.

Rectification. Three very different current–voltage (I – V) curves are shown for **1** (Figures 11–13). Figure 11 shows a relatively low rectification ratio and a higher current, obtained for an LB monolayer of **1** deposited on Au at 28 mN m^{-1} (i.e.,

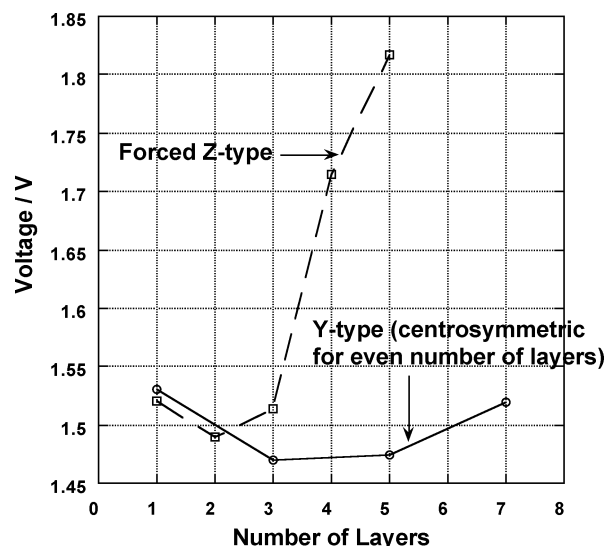


Figure 10. Volta potential for LB multilayers of **5** on a 150-nm-thick Au substrate.

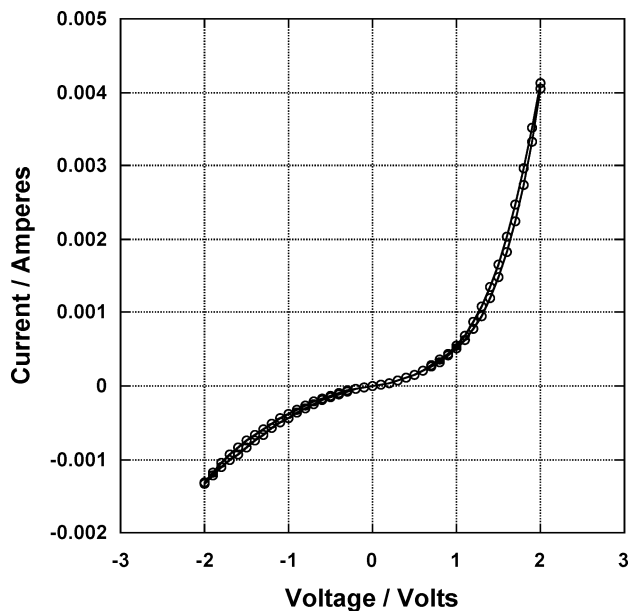


Figure 11. I – V curve for an “Au | LB monolayer of **1** | Au” sandwich, measured at room temperature (the LB transfer was performed at 17 $^\circ\text{C}$ and 28 mN m^{-1}). The maximum current is 4.12 mA at 2 V; the rectification ratio at ± 2 V is 3.03.

before the collapse point). Figure 12 shows a very high rectification ratio, but very low current, obtained for an LB monolayer of **1** deposited on Au beyond the collapse point, at 35 mN m^{-1} . Most pads of **1** show an I – V curve like Figure 11; the high rectification ratio of Figure 12 is seen less frequently. Because all resistances from Au to Ga/In pad to wires to current meter are in series, the overall current can (and does) vary from pad to pad. Not all junctions show asymmetries as large as that in Figure 12. Some junctions show very little asymmetry.

This variation of rectification has been reported on previously in great statistical detail, both for “Al | monolayer | Al” sandwiches⁵ and for “Au | monolayer | Au” sandwiches.⁸ Hence, here we record simply that we see a similar variation.

An interesting juxtaposition of two I – V curves for **1** is seen in Figure 13: at negative bias the intercepts are nearly equal (-1.9 and -2.0 V) beyond the film collapse point (where the transition moments for band C are in the plane of the film). In contrast, there is a 0.3 V difference between the intercepts for

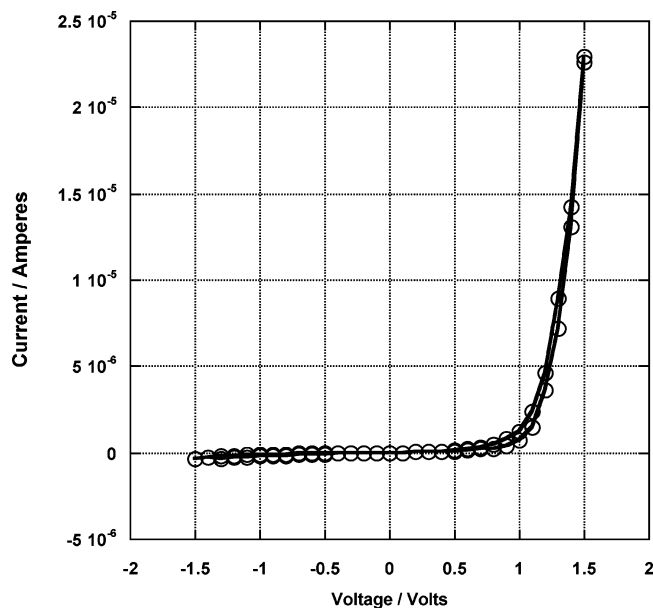


Figure 12. I – V curve for an “Au | LB monolayer of **1** | Au” sandwich, measured at room temperature (the LB transfer was performed at 17 °C and 35 mN m^{−1}). The maximum current is 22.9 μA at 1.5 V; the rectification ratio at ±1.5 V is 64.5.

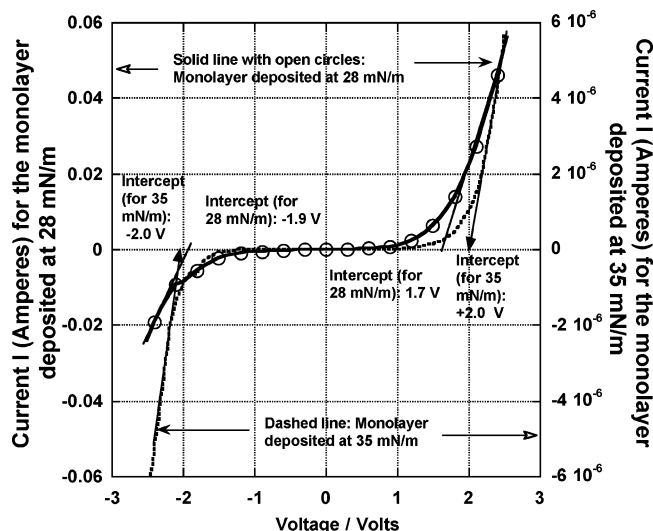


Figure 13. I – V curve at room temperature for two “Au | LB monolayer of **1** | Au” sandwiches, one deposited at 28 mN m^{−1} (solid line with open circles; current scale is on left), the other deposited at 35 mN m^{−1} (dashed line; current scale is on right). The intercepts of the slopes at zero current are at 1.7 and −1.9 V (for the film before collapse), and 2.0 and −2.0 V (for the film beyond collapse).

the film before collapse (where the transition moment of band B is normal to the film), at positive biases; this 0.3 V difference may be the signature of a Schottky barrier.

When the voltage range exceeds ±2.5 V, the I – V curves for **1** become more symmetric for films transferred either before (28 mN m^{−1}) or beyond (35 mN m^{−1}) the collapse point: this incipient symmetry is probably due to bias-induced molecular reorientation or chemical reaction.

Compound **5** also rectifies. Figure 14 shows a rectification ratio of 3.87. Figure 15 also shows that the films of **5** may withstand some number of cycles without significant decrease in rectification ratio. In one sandwich we recorded a rectification ratio of almost 100 at ±1.5 V, but this occurred only once, so it is not shown here.

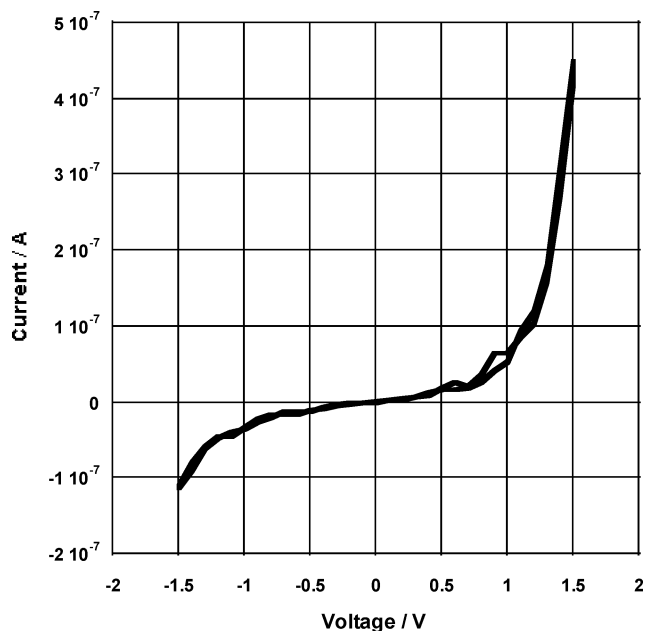


Figure 14. I – V curve for an “Au | LB monolayer of **5** | Au” sandwich, measured at room temperature (the LB transfer was performed at 17 °C and 28 mN m^{−1}). The maximum current is 450 nA at 1.5 V. The rectification ratio is 3.87 at ±1.5 V.

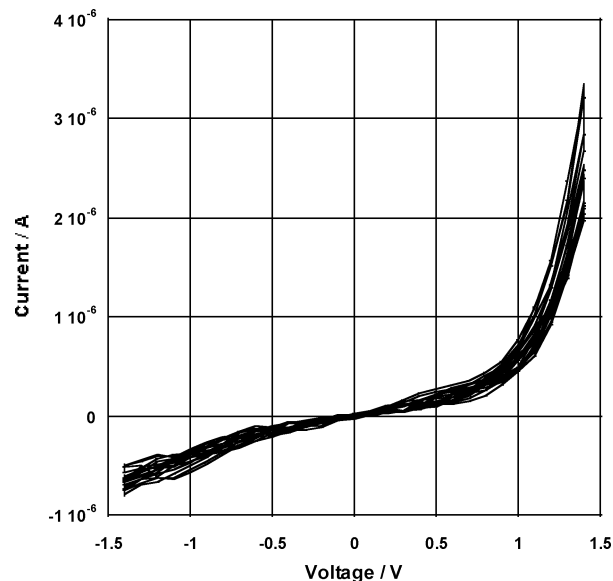


Figure 15. I – V curve for an “Au | LB monolayer of **5** | Au” sandwich, measured at room temperature (the LB transfer was performed at 17 °C and 28 mN m^{−1}). The rectification ratio remains fairly unchanged for 10 voltage sweeps.

As reported earlier for **1**,⁵ some “Au | monolayer of **5** | Au” sandwiches do not rectify at all, and the rectification does not usually persist at larger voltages (as discussed above for compound **1**). Figure 16 shows such a sandwich, which again shows unequal intercepts at zero current of −2.00 and +1.73 V, as a possible measure of small Schottky barriers (0.27 eV) at the “molecule | Au” interfaces, possibly caused by the large molecular dipoles and IVT transition dipoles normal to the film.

Compound **6** was studied as a SAM on Au, but the film was less compact, with pinholes, and all measured “Au | SAM of **6** | Au” pads were unfortunately short-circuited. Regrettably, time did not permit an STM study of a SAM of **6** on Au.

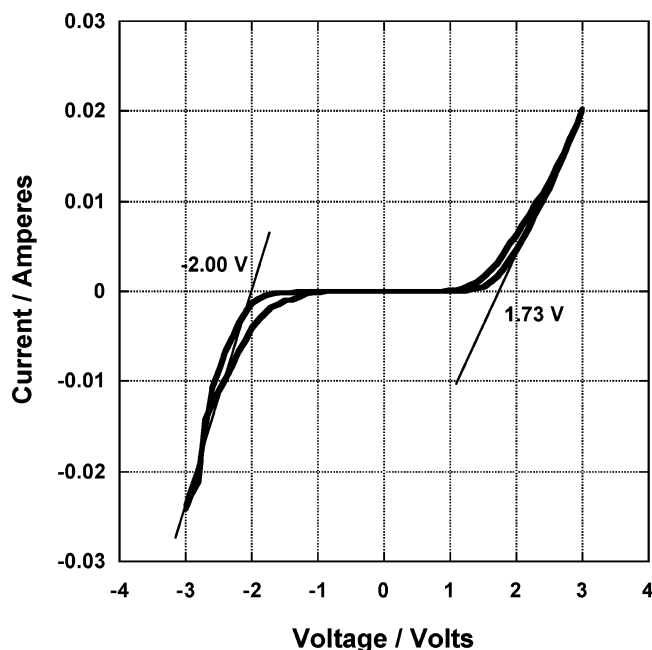


Figure 16. I - V curve for an "Au | LB monolayer of **5** | Au" sandwich, measured at room temperature. No significant rectification is seen, but the zero-current intercepts are -2.00 and $+1.73$ V.

Discussion

The CV for **5**, as compared to **1**, shows that **5** is more easily reduced (reversibly) than **1** (by 0.073 V), but is more difficult to oxidize (irreversibly) than **1** (by 0.344 V). Semiempirical molecular orbital calculations for **1**⁴ have shown that the HOMO amplitudes are spread throughout the chromophore, while the LUMO is concentrated on the 3CNQ moiety (confirmed by EPR⁹). This agrees with the expectation that the higher electronegativity of F versus H should make **5** easier to reduce and harder to oxidize than **1**. The 0.073 V shift in the CV reduction peak, due to fluorination of the 3CNQ ring, is considerably smaller than the 0.4 V shift to more positive reduction potentials upon fluorinating TCNQ to TCNQF₄; a possible shift in onset of the rectification for **5** versus **1** of 0.07 V, due to the lowering of the LUMO level, is too small to detect with the present instrumentation.

In the UV-vis spectrum of an LB monolayer of **1**, band A is attributed to an intramolecular π - π^* or n - π^* transition (which is less likely to be polarized), while band B at 530 nm has a transition moment normal to the plane of the monolayer, and band C at 570 nm has a transition moment in the plane of the monolayer.

We remind ourselves that polarized spectroscopy of a single crystal of P-3CNQ, **2**²⁶ revealed an intermolecular CT maximum at $12\,400\text{ cm}^{-1} = 806\text{ nm} = 1.54\text{ eV}$ and an intramolecular CT (or IVT) at $18\,600\text{ cm}^{-1} = 538\text{ nm} = 2.31\text{ eV}$.²⁶

The polarized absorption data (Figure 6) clearly indicate that band B (peak at 530 nm) is an intramolecular CT (or IVT) band, polarized along the direction from quinolinium to 3CNQ: indeed, if the transition moment vector forms an angle of 45° with the normal to the film for any individual molecule, then the LB transfer would provide domains of molecules of **1**, oriented randomly isotropically, to span a cone of half-angle 45° : the sample-average vector will be normal to the film, as observed. Band C (peak at 570 nm) is an intermolecular CT band, with a resultant vector in the plane of the film.

What is unusual is that bands B and C do not occur together in a film deposited at any given pressure (Figure 6). This means

that, as the pressure increases, the IVT at 530 nm is "turned off". The zwitterionic character of the film is the same at the two film pressures; the film thickness is almost the same ($24.0 \pm 1.0\text{ \AA}$ versus $25.6 \pm 1.0\text{ \AA}$). The disappearance of band B and the appearance of band C may occur by a sudden increase of the intramolecular twist angle θ (see Figure 1), made possible by the low energy barrier to rotation (see Figure A of the Supporting Information for a PM3 conformational energy calculation of the methyl analogue of compound **5**). Band C would involve intermolecular CT between the 3CNQ moiety of one molecule and the quinolinium moiety of the molecule lying next to it in the plane: this would explain why the transition moment of band C lies in the plane of the film.

Our results are in minor disagreement with a recent report that **1** has a noncentrosymmetric LB phase with strong second harmonic generation (SHG) and a sharp "J-aggregate" band at 563 nm ²⁷ (we would say an intramolecular band at 530 nm), and also has two centrosymmetric LB phases with weak or vanishing SHG intensity, and absorption bands centered at about 610 and 670 nm ²⁷ (these, we would say, are J-aggregate bands).

We had claimed⁴ that there was no NMR evidence for **1** of a temperature-dependent change in a twisted-internal-charge-transfer complex at high temperature, which had been suggested theoretically.²⁸ This is now known to be partially incorrect: the NMR spectrum of a recently synthesized sample of **1** does give only one rotamer at 330 K , as stated,⁴ but, at room temperature, shows a minority rotamer (or association dimer) ($\sim 10\%$): the separate NMR peaks from this (presumed) minority rotamer (or association dimer) disappear upon heating the solution to 330 K . This minority rotamer (or association dimer) may not exhibit IVT at 300 K and therefore may not contribute to the rectification signal. The association dimer would contribute to rectification.

In summary, we now claim that at the higher deposition pressure, beyond the collapse point (35 mN m^{-1}), the molecules undergo a slight compression, and change the twist angle θ from maybe 30° to maybe 90° , lose the intramolecular IVT B band at 530 nm and acquire a new intermolecular CT band, C, at 570 nm . The two different positions of the CT band in the spectra may also be due to the different orientations of the molecular dipoles.

The 1.5 eV downward shift in the XPS band edge between compounds **1** and **5** (making **5** more difficult to oxidize than **1**) is in agreement with the more electronegative F atoms moving the HOMO to more negative energies (versus vacuum), and with the sign of the $+0.347\text{ V}$ shift in the first oxidation observed in solution. An exact match is not expected because oxidation and reduction energies in solution are masked by considerable solvent-solute interactions.

Thus, the experimental data strongly suggest that both the HOMO and LUMO of **5** are lowered, with respect to the vacuum level, when compared to **1**. An increase in the ionicity of **5**, relative to **1**, was predicted.¹⁵

The shift in Volta potentials (from approximately constant with layer number for almost centrosymmetric Y-type deposition to almost linear with layer number for acentric forced Z-type deposition, Figure 10) is a reassuring confirmation that stacking layers of dipoles oriented all the same way, from layer to layer, will linearly increase the electric polarization of the multilayer.

The rectification of **1** has been reported extensively.^{4-8,29,30} The new result for **1** exhibited in Figure 11 is unremarkable: if the polarization of the IVT band shows molecular dipoles oriented along the normal to the film plane, then a two-level model of rectification, by a modified Aviram-Ratner mechanism⁴

explains what we see. The rectification ratio is not as impressive as has been seen sometimes, and a variation in rectification ratios for **1** has been observed (but not explained) previously.⁵

The I – V curve of Figure 12 shows low currents, and a very high rectification ratio. But this film was deposited at 35 mN m⁻¹ [at which pressure the CT transition moments are oriented in the plane of the film (Figure 6)]; if these transition dipoles are involved in the mechanism of rectification,⁴ then the film should not rectify at all. Indeed, LB monolayers of benzothiazolium 3CNQ compounds showed no rectification, presumably because the molecular dipoles in these molecules (presumably parallel to the optical transition dipoles) were oriented in the plane of the film.³¹ There are two alternative explanations for the conundrum: (1) the formation of the “Au | monolayer of **1** | Au” pad somehow allowed a relaxation of the molecules after film transfer, so the molecules lost the 570 nm C band, reacquired the 530 nm IVT B band absorption, and rectified by the two-level Aviram–Ratner mechanism; or (2) the rectification in **1** can be explained by a one-level model¹² rather than the two-level model.⁴

Molecule **5** rectifies as an LB monolayer (Figures 14 and 15), with onsets of asymmetry around 1 V. A comparison, for molecules **1** and **5**, of the “onset voltage”, at which asymmetric currents first appear, would have been interesting but was not possible, given the scatter of the results obtained so far. For molecule **1**, the decay of the rectification ratio was attributed to a possible rearrangement of an ordered LB monolayer with huge dipoles under the intense external electric field.^{4,8}

The expected greater ionicity of **5**, compared to **1**,¹⁵ did not yield a clear signature in the relative rectification behavior of the two molecules.

Self-assembly of **6** onto an Au electrode yielded a less compact film (with pinholes), so macroscopic Au pads could not be used to measure its electrical properties in the usual manner.

Conclusions

The polarization of charge-transfer bands in LB multilayers of **1** has been established: band B with a peak at 530 nm, obtained at lower film pressures at film transfer, is intramolecular (IVT), and the band with peak at 570 nm, obtained at higher film pressures, is intermolecular. In contrast, LB multilayers of **5** have a single IVT band with a peak at 504 nm at all film deposition pressures. The LB monolayer of **5**, sandwiched between Au electrodes, is also a unimolecular rectifier.

Acknowledgment. This work was supported in Tuscaloosa by grants from the United States National Science Foundation (DMR-01-20967 and DMR-00-95215) and in Kyoto by a grant-in-aid from the Japanese Society for the Promotion of Science. Discussions with Dr. Archana Jaiswal were very helpful. This paper is dedicated to the memory of Prof. Ian Robert Peterson (1945–2005), who left us too soon: we miss him and vow to maintain his impeccable standards of scientific honesty and decency.

Supporting Information Available: Synthesis details, theoretical calculations, and UV–vis spectra. This material is available free of charge via the Internet at <http://pubs.acs.org>.

References and Notes

- (1) Metzger, R. M. *Acc. Chem. Res.* **1999**, *32*, 950–957.
- (2) Metzger, R. M. *Chem. Rev.* **2003**, *103*, 3803–3834.
- (3) Metzger, R. M. *Chem. Rec.* **2004**, *4*, 291–304.
- (4) Metzger, R. M.; Chen, B.; Höpfner, U.; Lakshmikantham, M. V.; Vuillaume, D.; Kawai, T.; Wu, X.; Tachibana, H.; Hughes, T. V.; Sakurai, H.; Baldwin, J. W.; Hosch, C.; Cava, M. P.; Brehmer, L.; Ashwell, G. J. *J. Am. Chem. Soc.* **1997**, *119*, 10455–10466.
- (5) Vuillaume, D.; Chen, B.; Metzger, R. M. *Langmuir* **1999**, *15*, 4011–4017.
- (6) Chen, B.; Metzger, R. M. *J. Phys. Chem. B* **1999**, *103*, 4447–4451.
- (7) Xu, T.; Peterson, I. R.; Lakshmikantham, M. V.; Metzger, R. M. *Angew. Chem., Int. Ed.* **2001**, *40*, 1749–1752.
- (8) Metzger, R. M.; Xu, T.; Peterson, I. R. *J. Phys. Chem. B* **2001**, *105*, 7280–7290.
- (9) Baldwin, J. W.; Chen, B.; Street, S. C.; Konovalov, V. V.; Sakurai, H.; Hughes, T. V.; Simpson, C. S.; Lakshmikantham, M. V.; Cava, M. P.; Kispert, L. D.; Metzger, R. M. *J. Phys. Chem. B* **1999**, *103*, 4269–4277.
- (10) Xu, T.; Morris, T. A.; Szulcowski, G. J.; Amaresh, R. R.; Gao, Y.; Street, S. C.; Kispert, L. D.; Metzger, R. M.; Terenziani, F. *J. Phys. Chem. B* **2002**, *106*, 10374–10381.
- (11) Kwon, O.; McKee, M. L.; Metzger, R. M. *Chem. Phys. Lett.* **1999**, *313*, 321–331.
- (12) Peterson, I. R.; Vuillaume, D.; Metzger, R. M. *J. Phys. Chem.* **2001**, *A105*, 4702–4707.
- (13) Krzeminski, C.; Delerue, C.; Allan, G.; Vuillaume, D.; Metzger, R. M. *Phys. Rev.* **2001**, *B64*, 085405.
- (14) Terenziani, F.; Painelli, A.; Girlando, A.; Metzger, R. M. *J. Phys. Chem. B* **2004**, *108*, 10743–10750.
- (15) Saito, G.; Chong, C.-H.; Makihara, M.; Otsuka, A.; Yamochi, H. *J. Am. Chem. Soc.* **2003**, *125*, 1134–1135.
- (16) Ashwell, G. J.; Dawney, E. J. C.; Kuczyński, A. P.; Szablewski, M.; Sandy, I. M.; Bryce, M. R.; Grainger, A. M.; Hasan, M. J. *J. Chem. Soc., Faraday Trans.* **1990**, *86*, 1117–1121.
- (17) Ashwell, G. J.; Jeffries, G.; Dawney, E. J. C.; Kuczyński, A. P.; Lynch, D. E.; Gongda, Y.; Bucknall, D. G. *J. Mater. Chem.* **1995**, *5*, 975–980.
- (18) Bell, N. A.; Bradley, C. S.; Broughton, R. A.; Coles, S. J.; Hibbs, D. E.; Hursthouse, M. B.; Ray, A. K.; Simmonds, D. J.; Thorpe, S. C. *J. Mater. Chem.* **2005**, *15*, 1437–1445.
- (19) Metzger, R. M.; Heimer, N. E.; Ashwell, G. J. *Mol. Cryst. Liq. Cryst.* **1984**, *107*, 133–149.
- (20) Baldwin, J. W.; Amaresh, R. R.; Peterson, I. R.; Shumate, W. J.; Cava, M. P.; Amiri, M. A.; Hamilton, R.; Ashwell, G. J.; Metzger, R. M. *J. Phys. Chem.* **2002**, *B106*, 12158–12164.
- (21) Metzger, R. M.; Baldwin, J. W.; Shumate, W. J.; Peterson, I. R.; Mani, P.; Mankey, G. J.; Morris, T.; Szulcowski, G.; Bosi, S.; Prato, M.; Comito, A.; Rubin, Y. *J. Phys. Chem. B* **2003**, *107*, 1021–1027.
- (22) Honciuc, A.; Jaiswal, A.; Gong, A.; Ashworth, K.; Spangler, C. W.; Peterson, I. R.; Dalton, L. R.; Metzger, R. M. *J. Phys. Chem. B* **2005**, *109*, 857–871.
- (23) Emge, T. J.; Maxfield, M. R.; Cowan, D. O.; Kistenmacher, T. J. *Mol. Cryst. Liq. Cryst.* **1981**, *65*, 161.
- (24) Chappel, J. S.; Bloch, A. N.; Bryden, W. A.; Maxfield, M.; Poehler, T. O.; Cowan, D. O. *J. Am. Chem. Soc.* **1981**, *103*, 2442–2443.
- (25) Otsuka, A. Unpublished results.
- (26) Akhtar, S.; Tanaka, J.; Metzger, R. M.; Ashwell, G. J. *Mol. Cryst. Liq. Cryst.* **1986**, *139*, 353–364.
- (27) Ashwell, G. J.; Tyrell, W. D.; Whitman, A. J. *J. Am. Chem. Soc.* **2004**, *126*, 7102–7110.
- (28) Broo, A.; Zerner, M. C. *Chem. Phys.* **1996**, *196*, 423–426.
- (29) Ashwell, G. J.; Sambles, J. R.; Martin, A. S.; Parker, W. G.; Szablewski, M. *J. Chem. Soc., Chem. Commun.* **1990**, 1374–1376.
- (30) Martin, A. S.; Sambles, J. R.; Ashwell, G. J. *Phys. Rev. Lett.* **1993**, *70*, 218–221.
- (31) Hughes, T. V.; Mokijewski, B.; Chen, B.; Lakshmikantham, M. V.; Cava, M. P.; Metzger, R. M. *Langmuir* **1999**, *15*, 6925–6930.